Temporal Dynamics of Land Surface Temperature From Landsat TIR Time Series Images

Peng Fu and Qihao Weng, *Member, IEEE*

***Abstract*—Land surface temperature (LST) is a valuable parameter in studies of surface energy balance, landscape thermal patterns, and human–environment interactions. An effective way to quantify the LST dynamics over spatial and temporal domains is to utilize the consistent Landsat thermal infrared (TIR) data since 1982. Currently, only a small proportion of studies utilized the Landsat TIR data for investigating both the intra- and interannual LST variations. The objectives of the study are to provide statistical evidence for the existence of the annual temperature cycle (ATC) and to develop a decomposition technique to explore landscape thermal patterns by land cover. Eighty-two cloud-free TIR images of Los Angeles County from Landsat TM between 2000 and 2010 were collected and consistently calibrated to the LSTs. The LSTs were then analyzed by the Lomb–Scargle periodogram technique to test whether the time series LSTs showed rhythmic patterns and by a decomposition model to analyze the intra- and interannual landscape thermal patterns. The periodogram analysis confirmed that ATC was statistically significant with the periodic time of 362 days. Furthermore, sensitivity analysis showed that the Lomb–Scargle technique can still discover the ATC with the difference of up to five days, even when the number of images decreased to 60. Based on the periodogram analysis, a decomposition model was initialized to disassemble the time series LSTs into seasonality and trend components for comparisons among land covers. Results suggested that the developed areas exhibited relatively low seasonal amplitude of 11.7 K, while largest mean annual LST value is 302.8 K. The difference of the averaged trend component between urban and other land covers reached 1.1 K over the decade. Future research may be directed in dealing with the time-varying seasonality component for better quantifying the thermal patterns.**

***Index Terms*—Annual temperature cycle (ATC), decomposition, land surface temperature (LST), thermal patterns.**

I. Introduction

LAND surface temperature (LST), which is routinely estimated from remotely sensed thermal infrared (TIR) data to represent the skin temperature of the Earth's surface, is an indispensable parameter in analyzing landscape thermal patterns, modeling surface energy balance, and quantifying evapotranspiration for water management [1]–[3]. It has been reported that time series LST conditions are important in analyzing cardiorespiratory mortality and the outbreak and propagation of vectorborne disease [4], [5]. In addition, it remains a scientific issue to estimate the urban heat island parameters from the time series TIR imagery to gain a better understanding of the urban thermal landscape [6]. Therefore, estimation of LST and its temporal patterns can not only facilitate the understanding thermal characteristics but also benefit the studies of public health.

Rhythmic patterns occur in all land surface processes dominated by the annual cycle caused by the changes in solar radiation. Previous studies mainly focused on LST dynamics of the annual cycle, usually referred as $A(t)\cos(2\pi t+\theta)$, since seasonality is dependent, within a phase lag, on the yearly cycle of insolation at the top of atmosphere aroused by the Earth's changing position [7]. Nevertheless, solar radiation reaching land surface is not the same as that received at the top of atmosphere, owing to the nonlinear response of Earth's climate and environmental system [8]. Urbanization processes, particularly the land cover changes, which are characterized by the increase in sensible heat fluxes, the decrease in latent heat fluxes, and an extra component of anthropogenic heat discharge, further complicated the nonlinear responses.

The fast Fourier transform (FFT) is a popular computational technique to identify rhythmic patterns by isolating periodicities from searching for sharp peaks in the ordinary periodograms calculated from the Fourier transform of a time series. Van De Kerchove *et al.* [9] differentiated short-term weather components from strong and climate-related periodic patterns by applying the FFT technique to both daytime and nighttime Moderate Resolution Imaging Spectroradiometer (MODIS) data to unfold the spatiotemporal variations in the Russian Altay Mountains. An alternative way to FFT is to use a parametric model with fixed angular frequency, amplitude, and constant trend to fit the time series data. Bechtel [1] and Weng and Fu [10] used the sinusoidal model to analyze the annual temperature cycle (ATC) of LSTs. The ATC model, however, can only capture the averaged LST variation within individual years, and ignore gradual or abrupt changes over a decadal year. Therefore, new methods are needed to deal with the unevenly distributed time series data to understand both the intra- and interannual LST dynamics.

The Landsat consistent records of the thermal state of Earth's surface since 1982 represent hitherto the only long-term TIR data with spatial scales appropriate for urban studies globally. At present, only a small portion of studies emphasize the importance of historical Landsat TIR data for investigating both the intra- and interannual landscape thermal patterns [1], [10]. Possible reasons for the underutilization of the Landsat archive may be imputed to the following aspects: 1) although the open access data policy allows for the procurement of Landsat data held by the U.S. Geological Survey (USGS) free

Manuscript received April 6, 2015; revised May 28, 2015; accepted June 26, 2015.

The authors are with the Center for Urban and Environmental Change and Department of Earth and Environmental Systems, Indiana State University, Terre Haute, IN 47809 USA (e-mail: qweng@indstate.edu).

Color versions of one or more of the figures in this paper are available online at http://ieeexplore.ieee.org.

Digital Object Identifier 10.1109/LGRS.2015.2455019

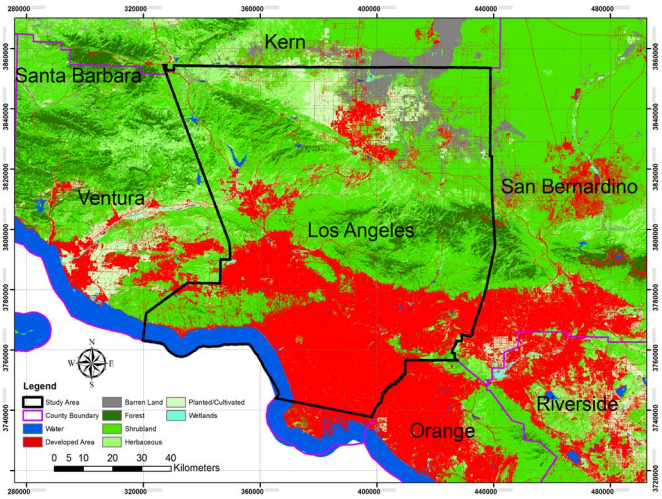

Fig. 1. Geographic location of the study area.

of charge, an effort to completely and consistently calibrate the archive into absolute surface radiometric temperature is still in progress (http://landsat.usgs.gov/). Lack of atmospherically compensated and calibrated Landsat thermal radiance/LST operational products limits the use of Landsat archive for characterizing landscape thermal patterns over a long time scale. 2) Technically, there exist difficulties in analyzing the time series Landsat TIR data. In spite of the constant sampling frequency of the satellite sensors (e.g., 16 days for Landsat), the recorded data may be irregularly available because of cloud contamination and poor atmospheric conditions. This irregularity poses a great challenge in extracting LST periodic patterns with known and acceptable confidence level using traditional statistics and techniques that (e.g., FFT) are only applicable for evenly distributed data. In this letter, we attempted, by selecting Los Angeles as the study area and by utilizing Landsat TIR image series; 1) to provide the statistical evidence for the existence of periodic patterns within LSTs; 2) to develop a new method to decompose unevenly spaced LST time series into a seasonal, a trend, and a remainder component; and 3) to analyze temporal LST patterns among land covers.

II. Study Area and Data Source

A. Study Area

The study area consists of nearly the whole Los Angeles County, California, except for the southern part and two offshore islands, namely, the Santa Catalina Island and the San Clemente Island (see Fig. 1). This area comprises geographically diverse regions, such as hilly mountains, deep valleys, ocean coastlines, forests, lakes, rivers, and barren land. The National Land Cover Database (NLCD) 2006 identified eight land cover types in the study area, i.e., water, developed, barren, forest, shrubland, herbaceous, planted/cultivated, and wetlands. The selection of Los Angeles County is due to its greater chance to acquire clear-sky images than other megacities, such as New York, Chicago, or Houston, to facilitate the subsequent time series analysis. The area has a subtropical Mediterranean-type climate with a dry summer and moist winter. The average maximum air temperature is 29 °C in August and 20 °C in January based on the weather records from the Downtown University of Southern California campus.

TABLE I
Mean Value of Periodic Time Identified With the Number of Images Ranging From 250 to 40 (Unit: Days)

Image Number	250	230	210	190	170	150
Periodic time	365.0	365	364	364	364	363
Image Number	130	110	90	80	60	40
Periodic time	363	362	361	360	360	321

B. Data Sources

An operational LST product from Landsat TM/ETM+ archive will definitely benefit the current research. Considering that the product is still in progress, an alternative way to derive LST maps is to use the NASA Correction Parameter Calculator [11], which uses the National Centers for Environmental Prediction (NCEP) modeled atmospheric global profiles interpolated to a particular date, time, and location as input for the MODTRAN radiative transfer code and a suite of integrative algorithm to infer the upwelling and downwelling radiances and site-specific transmission. The data used in the research were from the Thematic Mapper (TM) sensor on board Landsat 5 from the period of February 3, 2000 to December 31, 2010. The level L1T product was downloaded from the Landsat archive through the USGS website. Only clear-sky images of the study area were selected according to the image metadata. Eventually, a total of 82 scenes available from the Landsat archive was utilized for the analysis. The mean acquisition time was 18:13 P.M. UTC (10:13 A.M. local time) with the standard deviation of 6 min.

Sensitivity tests were performed to show how the number of images could affect the ability of the Lomb–Scargle technique (Section III-B) to discover the periodic patterns. The data for the sensitivity analyses came from simulation. First, the seasonal component was produced by a sinusoidal model with constant amplitude value and angular frequency. This sinusoidal function has been shown to perform well for modeling ATC [1], [10]. Second, the trend component was created by using a linear change. The remainder item was derived by using a random number generator that followed a normal distribution $N(\mu = 0, \delta = x)$. The δ value was set to 1 K, according to [12]. Final simulation data were generated by summing the simulated seasonal, trend, and remainder components. Since the simulation followed the decomposition model in Section III-B, the RMSE between the simulated LSTs and remote sensing data was expected to range from 1.5 to 5.3 K for different land covers (see Table II). Without cloud contaminations, roughly the number of clear-sky Landsat images would be 250 over 10 years. The uneven distribution was produced by the random selection from the 250 dates. The total number of date points selected was from 230 to 40 (see Table I). In each scenario (e.g., the number of images is 150), the procedure to generate the uneven distribution and to identify the periodic time were repeated for 1000 times. The mean value of the periodic time identified from the 1000 times was recorded.

III. Methodology

Rapid growth of urbanization-induced land use and land cover changes may impact LST variations at the local, the regional, and even the global scale. This may blur both the intra- and interannual LST variations. Therefore, it is necessary

to conduct the statistical hypothesis testing for LST periodicity and to model the interannual variations by using a decadal year data. First, TM imagery data were subject to the preprocessing operations, including subset, atmospheric calibration, and computation of LSTs. Details for the LST computation can be found in [10]. The LST time series were then analyzed by using the Lomb–Scargle periodogram technique (also known as least square spectral analysis) [13], [14] and by using the decomposition method. Section III-A and B present the details of the statistical hypothesis testing technique and the decomposition method.

A. Lomb–Scargle Periodogram for Periodicity

Although the rhythmic pattern within LST variations has been modeled as a sinusoidal function [1], [10], previous studies did not provide any statistical analysis for the constant annual frequency, i.e., 365 days. The difficulty to search for the periodicity of LST is exacerbated by the unevenly distributed images. The traditional decomposition technique, such as FFT, cannot be used to identify the periodic patterns from the unevenly spaced time series data. The Lomb–Scargle periodogram was proposed in this study as the statistical hypothesis testing technique to search for possible periodic components. For an LST value at a pixel location observed at time t_i, we denote the time series data by $Y(t_i)$ for $i = 1, 2, 3, \ldots, N$. To model $Y(t_i)$ for periodicity, we have

$$Y(t_i) = S(t_i) + \varepsilon(t_i) \tag{1}$$

where $S(t_i)$ is a periodic function with a positive period T such that $S(t_i) = S(t_i + T)$ for all t_i; and $\varepsilon(t_i)$ is assumed as a sequence of normal random errors with mean 0 and homogeneous variance [13]. Unlike the Fourier TRANSFORM, in which the Fourier frequencies are used, the Lomb–Scargle periodogram analysis assumes that there are M test frequencies $f_1, f_2, \ldots, f_M$ and their corresponding angular frequencies are $\omega = 2\pi f_j$, for $j = 1, 2, \ldots, M$. The null distribution of the Lomb–Scargle periodogram $Z_j = P(\omega_j)$ at a given frequency ω_j is exponentially distributed [13], i.e., the cumulative distribution function is

$$F(z) = P(Z_j < z) = 1 - e^{-z}. \tag{2}$$

In the present study, the null hypothesis is that LST time series is nonperiodic versus the alternative one that it is periodic. Thus, the observed statistical significance level (p-value) of testing the null hypothesis that such a peak in Lomb–Scargle periodogram is due to chance, is calculated by (3) that supposes there are M independent frequencies. Thus

$$\Pr = p - \text{value} = 1 - (1 - e^{-z})^M. \tag{3}$$

The advantage of Lomb–Scargle technique lies in its ability to deal with irregular time series data, as well as to provide the statistical significance for the identified rhythmic patterns. Nevertheless, the ability of Lomb–Scargle technique to identify the periodic patterns can change with the number of images used in the analysis. As such, sensitivity tests were performed to show how the number of images used can affect the ability of the Lomb–scargle technique to discover the periodic patterns.

B. LST Decomposition

The periodicity patterns identified from the periodogram analysis provide the intra-annual patterns. It ignores, however, the interannual gradual change over a decadal year. The utilization of the decomposition model is to investigate both the periodic pattern and the gradual change within the LSTs. A breakdown scheme was developed to disassemble LST data into a seasonal, a trend, and a remainder component using (4). This equation is initialized based on the input from the periodogram analysis for the determination of the number of periodic patterns [variable n in (4)] used for the modeling procedure, i.e.,

$$y = \sum^{n} [a_i * \cos(w_{1i}t) + bi * \sin(w_{2i}t)] + c_1 + c_2 t + \varepsilon \tag{4}$$

where a_i and b_i are the coefficients of the seasonal component; w_1 and w_2 are the frequencies of the periodic patterns within the LST variations; n represents the number of sinusoidal functions and is dependent on the number of the periodic patterns identified by the Lomb–Scargle technique; c_1 and c_2 are the coefficients of the trend component used to represent the gradual changes for the LST variations; t is the date; and ε is the remainder component, which can be computed from the residuals after subtracting the model values from the real observations. The decomposition scheme was applied to all the image pixels. The LST landscape patterns were characterized among all the land covers, based on the seasonality and trend components. The rationale of the decomposition model is that the intra- and interannual components can be well captured by the sinusoidal and linear functions. First, the Lomb–Scargle technique can provide the number of and the angular frequency for the rhythmic patterns and thus be useful for modeling the seasonality component. A linear change is used as an approximation to complex phenomena to extract basic features of the data [15].

IV. Results

A. Rhythmic Patterns Analysis

The application of the Lomb–Scargle periodogram to the time series LST images produced estimates of power density, periodic frequency, and the corresponding statistical significance level for individual pixels. The defined power density of the Lomb–Scargle has the ability to make the periodogram analysis invariant to the shift of the origin time and equivalent to the least square fitting process [13]. To illustrate the usefulness of the three parameters in analyzing the periodic patterns of LST time series, an urban pixel with UTM coordinate (Zone 11N, Easting 3865953.603, Northing 3751873.495, unit in meters) was selected. Its temporal LST values and periodogram results are shown in Fig. 2.

Panel (a) displays the LST variations between 2000 and 2010. Since the defined power density was invariant to the origin of the time, the first day of 2000 was considered as day 1, from which the day number of all images was computed. Because the Landsat revisit time is 16 days, the maximum frequency for the periodogram analysis was set to 0.031 (1/32), i.e., the sampling Nyquist frequency. In the current study, this operation seemed to be unnecessary, since the periodogram results in panels (b) and (c) only provided frequency up to

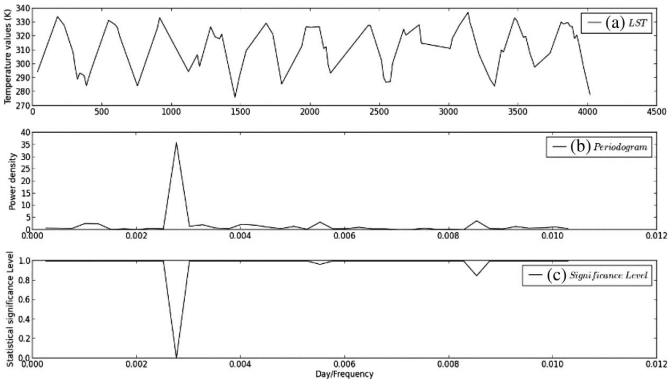

Fig. 2. (a) LST observations: the first day of 2000 is day 1, from which the day numbers of all images is computed. The periodogram results are (b) power density and (c) the statistical significance level.

around 0.011. This was due to the inherent capability of Lomb–Scargle technique to determine the frequency range under the limit of the maximum frequency. In panel (b), there are several local peaks, occurring at frequency 0.00275 (period 362), 0.00552 (period 181), and 0.00853 (period 117), respectively. If these peaks were statistically significant, then the three periodic times essentially corresponded to the frequencies of 1/365, 2/365, and 3/365 (annual, semiannual, etc.). Panel (c) provides the matching downward peaks for the statistical significance values, and the last two periodic times should be rejected at the significance level of either 0.05 or 0.01. Nevertheless, since the Lomb–Scargle is a statistical hypothesis testing technique, rejection did not mean that there were not semiannual and seasonal variations within the time series LSTs. Instead, the results suggested that the LSTs collected were inadequate in determining the semiannual and seasonal variations, although they could be used for isolating the annual LST variation at the significance level of 0.01 with a period of 362 days.

Weng and Fu [10] assumed that ATC had a period of 365 days rather than the 362 days identified in this study. To determine whether the difference was caused by data missing or was limited by the Landsat revisit interval, the simulated LST data were used with the periodic time set to 365 days (the annual magnitude was set at 15 K, the trend component at 0.001 K/day, the mean value at 295 K, and the remainder component at 1 K). The only parameter to be changed was the number of images preserved to test the tolerance ability of the Lomb–Scargle to data missing. The generation of the unevenly distributed data and the application of the Lomb–Scargle technique to the simulated data were performed 1000 times. Table I shows the results for the mean periodic time identified with the number of images ranging from 250 to 40. Overall, the detection capability of the periodogram technique decreased with fewer images. The periodic time was identifiable with as few as 60 images, but with a difference of five days in the period. The current study that used 82 cloud-free images to analyze the annual temperature patterns was therefore sufficient. The technique to identify the periodic patterns did not work well after the number of images was decreased to 40. Similar results were obtained by using different settings of the seasonal and trend components. Therefore, the difference in periodic time between the current study and that of Weng and Fu [10] was attributed to data missing caused by clouds and/or poor atmospheric conditions.

TABLE II
DECOMPOSITION OF THE LST VARIATIONS BY LAND COVERS

Land cover	a_1	b_1	*Magnitude*	c_1	c_2	*RMSE*
water	0.8	2.3	2.4	288.9	0.0008	1.5
developed	9.4	7.1	11.7	302.8	0.0012	5.4
barren	18.5	10.9	21.5	300.1	0.0010	3.9
forest	10.7	8.1	13.4	292.9	0.0009	3.6
shrubland	11.1	8.7	14.1	299.7	0.0008	4.8
herbaceous	15.2	8.5	19.9	296.5	0.0009	4.8
planted	16.3	11.4	18.4	297.3	0.0009	4.2
wetlands	9.6	7.1	11.9	293.7	0.0008	3.9

Note: The unit is Kelvin (K). a_1 and b_1 are the coefficients of the seasonal component, c_1 and c_2 are the coefficients for the trend component, *RMSE* represents the model fit error. The magnitude was computed based on the square root of the two coefficients of the seasonal component. The unit of c_2 is K/day.

B. Decomposition Analysis

The decomposition of the time series observations allows the examinations of LST patterns among land covers by introducing the seasonality and trend components. Since the periodogram analysis revealed only the annual periodic pattern, the number of periodic patterns [variable n in (4)] was set at 1. The modeling procedure was performed at the pixel level. The mean values of the seasonality and trend components by land cover are shown in Table II. The average RMSE for the model fit of all the land covers was 4.0 K with standard deviation of 1.1 K (see Table II). The RMSE value may be attributed to the assumption that the seasonality component was constant. The seasonality component may change over time because of land cover changes or climatic effects.

To demonstrate the necessity for including the trend component, the RMSE value between the predicted and observed LSTs for each land cover was computed based solely on the sinusoidal model. The averaged RMSE value for the model fit without the linear function was 5.3 K, which was larger than 4.0 K when both the seasonal and trend components were used, suggesting that the inclusion of the trend component was necessary. In addition, the Mann–Kendall test [16] was utilized, and the results demonstrated that the monotonic trend for each land cover was statistically significant at the level of 0.01.

The amplitude of the seasonality component by land cover was successfully retrieved, which ranged from 2.4 K (water), 11.7 K (developed), 11.9 K (wetland), 13.4 K (forest), 14.1 K (shrubland), 18.4 K (planted), 19.9 K (herbaceous), to 21.5 K (barren) (see Table II). As this parameter showed the stability of mean annual temperature, greater values indicated larger shifts from the mean temperature variations. Water exhibited the minimum temperature amplitude, and this was due to its large heat capacity. The seasonal amplitude of the developed area was 11.7 K, which was less than the land covers of wetland, forest, shrubland, planted, herbaceous, and barren. This suggested that the developed area may decrease the seasonal temperature variations. This was likely caused by the increase of anthropogenic heat release in the winter that raised the annual minimum temperature. Despite the low seasonal amplitude, developed areas showed the largest mean annual LST values of 302.8 K over the study period, revealing the notorious urban heat island phenomena.

The trend component is used to represent the interannual change or to show the long-term temperature tendency. Overall, all the land covers showed the upward trend, ranging from

0.0008 to 0.0012 K/day (see Table II). This was consistent with the increase trend derived from the air temperature anomalies considered to reflect the climate change [17]. LST and air temperature are different parameters in climate change assessment. The gradual trend change values derived from the air temperatures and LSTs were thus not the same. Compared with other land covers, developed area shows the highest increase trend over the decadal years (see Table II). This higher trend change in the urban areas may reflect that the urbanization-related changes, such as deforestation and other land cover changes, may increase the long-term LST trend. Based on the coefficients c_2 in Table II, the mean difference of trend component between urban and other land covers was 0.0003 K/day, or 1.1 K over the decade.

V. Discussion

The study aimed at decomposing the unevenly distributed time series Landsat LST data for characterizing landscape thermal patterns by land cover. To our knowledge, the existence of LST periodic pattern was first statistically confirmed, although previous studies had demonstrated the suitability of an ATC model to quantify thermal patterns. The Lomb–Scargle technique can be used for further exploring the periodic patterns involved in other biophysical parameters, such as NDVI and LAI, and even data from MODIS time series. The periodogram analysis not only can detect annual change but also shows the ability to isolate the periodic patterns at intraannual scales, depending on the availability of the data. If some of the biophysical parameters only show periodic patterns, they could be reconstructed from the remote sensing observations at even finer scales, such as from 16 days (Landsat revisit frequency) to a daily basis. The application of the Lomb–Scargle technique would be very useful, particularly for regions experiencing severe cloudy conditions.

The decomposition technique was developed to analyze the temporal landscape thermal patterns by land cover. The parametric decomposition technique assumed that the seasonality component was time constant, i.e., there was no change in the seasonality component over a decade. Such an assumption may be held over a decade since the ten-year data may not allow the identification of the change of seasonality. Nevertheless, if a longer time series of LST data was utilized, it would be more likely to detect changes in the seasonality due to land cover changes or climatic disturbance events. Based on much longer time series data, further efforts are therefore necessary to first divide the time series observations into different segments corresponding to different land covers before analyzing thermal patterns. The decomposition technique also shows potential in land cover change classification. Table II shows that different land covers have different seasonality and trend parameters. Land cover classification thus can be realized through the supervised classification technique (e.g., random forest) with inputs from the thermal parameters, i.e., a_1, b_1, c_1, c_2.

VI. Conclusion

This letter has proposed to use the Lomb–Scargle and the decomposition technique to explore the thermal characteristics over time. The error for the frequency estimation of the rhythmic patterns could be up to five days, following the decrease of the number of simulated time series points to 60 images. The parametric decomposition technique consisting of the seasonal, trend, and remainder components provides a unique way to examine both the intra- and interannual LST variations. Results suggested that the developed area had the largest mean annual temperature variation of 302.8 K, despite the relatively low seasonal amplitude of 11.7 K. A comparison analysis of the trend component between urban and other land covers revealed a mean difference value of 1.1 K from 2000 to 2010. Overall, the derived intra- and interannual parameters generally followed the land cover patterns and allowed for characterizing the landscape thermal patterns.

References

[1] B. Bechtel, "Robustness of annual cycle parameters to characterize the urban thermal landscapes," *IEEE Geosci. Remote Sens. Lett.*, vol. 9, no. 5, pp. 876–880, Sep. 2012.

[2] M. A. Friedl, "Forward and inverse modeling of land surface energy balance using surface temperature measurements," *Remote Sens. Environ.*, vol. 79, no. 2/3, pp. 344–354, Feb. 2002.

[3] M. C. Anderson, R. G. Allen, A. Morse and W. P. Kustas, "Use of Landsat thermal imagery in monitoring evapotranspiration and managing water resources," *Remote Sens. Environ.*, vol. 122, pp. 50–65, Jul. 2012.

[4] L. Liu *et al.*, "Associations between air temperature and cardio-respiratory mortality in the urban area of Beijing, China: A time-series analysis," *Environ. Health*, vol. 10, no. 1, pp. 51, May 2011.

[5] H. Liu and Q. H. Weng, "Enhancing temporal resolution of satellite imagery for public health studies: A case study of West Nile virus outbreak in Los Angeles in 2007," *Remote Sens. Environ.*, vol. 117, pp. 57–71, Feb. 2012.

[6] Q. Weng, "Thermal infrared remote sensing for urban climate and environmental studies: Methods, applications, and trends," *ISPRS J. Photogramm. Remote Sens.*, vol. 64, no. 4, pp. 335–344, Jul. 2009.

[7] D. J. Thomson, "The seasons, global temperature, and precession," *Science*, vol. 268, no. 5207, pp. 59–68, Apr. 1995.

[8] C. Qian, C. B. Fu, and Z. H. Wu, "Changes in the amplitude of the temperature annual cycle in China and their implication for climate change research," *J. Clim.*, vol. 24, no. 20, pp. 5292–5302, Oct. 2011.

[9] R. Van De Kerchove, S. Lhermitte, S. Veraverbeke, and R. Goossens, "Spatio-temporal variability in remotely sensed land surface temperature, and its relationship with physiographic variables in the Russian Altay mountains," *Int. J. Appl. Earth Observ. Geoinf.*, vol. 20, pp. 4–19, Feb. 2013.

[10] Q. Weng and P. Fu, "Modeling annual parameters of clear-sky land surface temperature variations and evaluating the impact of cloud cover using time series of Landsat TIR data," *Remote Sens. Environ.*, vol. 140, pp. 267–278, Jan. 2014.

[11] J. A. Barsi, J. R. Schott, F. D. Palluconi, and S. J. Hook, "Validation of a web-based atmospheric correction tool for single thermal band instruments," in *Proc. SPIE*, 2005, vol. 5882, p. 58820E.

[12] J. A. Sobrino *et al.*, "Land surface emissivity retrieval from different VNIR and TIR sensors," *IEEE Trans. Geoscience and Remote Sensing*, vol. 46, no. 2, pp. 316–327, Feb. 2008.

[13] J. D. Scargle, "Studies in astronomical time series analysis. II—Statistical aspects of spectral analysis of unevenly spaced data," *Astrophys. J.*, vol. 263, pp 835–853, Dec. 1982.

[14] N. R. Lomb, "Least-squares frequency analysis of unequally spaced data," *Astrophys. Space Sci.*, vol. 39, no. 2, pp. 447–462, Feb. 1976.

[15] A. Zeileis, C. Kleiber, W. Krämer, and K. Hornik, "Testing and dating of structural changes in practice," *Comput. Stat. Data Anal.*, vol. 44, no. 1/2, pp. 109–123, Oct. 2003.

[16] S. R. Esterby, "Review of methods for the detection and estimation of trends with emphasis on water quality applications," *Hydrol. Process.*, vol. 10, no. 2, pp. 127–149, Feb. 1996.

[17] M. Jin and R. E. Dickinson, "New observational evidence for global warming from satellite," *Geophys. Res. Lett.*, vol. 29, no. 10, pp. 39:1–39:4, May 2002.